Biochemistry and Biophysics Reports 40 (2024) 101858

Contents lists available at ScienceDirect

Biochemistry and Biophysics Reports

journal homepage: www.elsevier.com/locate/bbrep

LINC00261 triggers DNA damage via the miR-23a-3p/CELF2 axis to mitigate the malignant characteristics of ^{131}I-resistant papillary thyroid carcinoma cells

Qingyuan Tao [a,1], Xiaojin Li [b,1], Yanyan Xia [a], Bin Zheng [a], Yijun Yan [a], Songrun Wang [a], Li Jia [a,*]

[a] The Affiliated Hospital of Yunnan University (Yunnan Second People's Hospital), Nuclear Medicine, Kunming, Yunnan, 650021, China
[b] The Affiliated Hospital of Yunnan University (Yunnan Second People's Hospital), Central Laboratory, Kunming, Yunnan, 650021, China

ARTICLE INFO

Keywords:
LINC00261
^{131}I-resistant papillary thyroid carcinoma cells
miR-23a-3p
CELF2
DNA damage

ABSTRACT

Background: Long-chain non-coding RNA (LINC00261) in the treatment of papillary thyroid carcinoma (PTC) with ^{131}I is still unknown despite its proven anti-tumour effect in thyroid cancer (TC) and other types of cancer.
Methods: The database and RT-qPCR were used to analyze the expression level of LINC00261 in PTC and cell lines. PTC cells resistant to ^{131}I (TPC-1/R) were created through ongoing exposure to a lethal dose of ^{131}I, and a subcutaneous xenotransplantation model was developed using PTC mice. Bioinformatics analysis and dual-luciferase assays demonstrated the interaction between LINC00261, miR-23a-3p, and CELF2. RT-qPCR and Western blot were used to detect the expression of LINC00261, miR-23a-3p, and CELF2. Additionally, CCK-8, flow cytometry, immunofluorescence (IF), Western blot, and comet assay were employed to measure cell viability level and DNA damage.
Results: PTC cell lines exhibited a decrease in the expression of LINC00261. The growth and progression through the S-phase of TPC-1/R cells were suppressed by LINC00261, leading to increased apoptosis and DNA damage. The objective of LINC00261 was to regulate the axis of miR-23a-3p/CELF2. Downregulating LINC00261 enhances the growth and advancement of ^{131}I-resistant cells in the S-phase by activating the miR-23a-3p/CELF2 pathway while suppressing cell death and DNA harm. The miR-23a-3p/CELF2 axis activates DNA damage in ^{131}I-resistant PTC cells by LINC00261.
Conclusions: LINC00261 activates DNA damage in ^{131}I-resistant PTC cells caused by miR-23a-3p/CELF2 axis, improving the progression of cancer cells of PTC.

1. Introduction

In women, thyroid cancer (TC) has risen to become the fifth most prevalent form of cancer and the leading malignant tumour affecting the endocrine system. The incidence and mortality rates of this disease rising annually [1]. Over 80 % of all TCs are classified as papillary thyroid carcinoma (PTC), which represents the most prevalent malignant tumour affecting the thyroid. Due to its high propensity for metastasis, invasiveness, and poor prognosis, the mortality rates among patients are significantly increased [2]. At present, the management of TC primarily involves surgical removal and subsequent treatment with radioactive iodine (RAI, ^{131}I) therapy. The use of 131I as an established adjuvant treatment has been demonstrated to be beneficial for patients with TC [3]. Due to the propensity of PTC for local recurrence and distant metastasis, some patients with PTC remain unresponsive to ^{131}I therapy, thus classifying them as RAI refractory patients with a 3-year OS rate below 50 % [4]. Therefore, the objective of this study is to gain a deeper understanding of the molecular mechanisms underlying the resistance of PTC to ^{131}I, with the aim of identifying promising molecular targets.

Long non-coding RNAs (lncRNAs), defined as non-coding RNAs exceeding 200 bp in length, have been demonstrated to play a role in the regulation of a range of cellular biological processes [5]. LncRNA has emerged as a pivotal regulator of cancer biology. A number of research studies have indicated that lncRNA plays a crucial role in regulating the

* Corresponding author. The Affiliated Hospital of Yunnan University (Yunnan Second People's Hospital) Nuclear Medicine, No.176 Qingnian Road, Kunming, Yunnan, 650021, China.
E-mail address: jiali760318@126.com (L. Jia).
[1] These authors contributed to the work equally and should be regarded as co-first authors.

https://doi.org/10.1016/j.bbrep.2024.101858
Received 30 August 2024; Received in revised form 11 October 2024; Accepted 25 October 2024

progression of various illnesses, including TC progression [6]. Furthermore, evidence suggests that lncRNA may represent a promising target for therapeutic intervention in TC [7,8]. In a study by Shi et al., 23 lncRNAs and mRNAs were identified as being aberrantly expressed in thyroid carcinoma and adjacent tissues [9]. Furthermore, lncRNA has the potential to influence the radiation response of patients following radiotherapy, thereby regulating the efficacy of the treatment [10]. The relationship between lncRNA and the progression of PTC has been established, demonstrating its ability to enhance the therapeutic efficacy of ^{131}I and ultimately leading to improved patient survival rates [11]. LncRNA 261 (LINC00261) is topic of considerable research interest, with evidence indicating its aberrant expression in a range of malignant human tumours, including pancreatic cancer (PC), gastric cancer (GC), lung cancer, and others [12-14]. In their study, Zhang and colleagues identified LINC00261 as a cancer suppressor, demonstrating its role in regulating numerous cancer-related biological processes, including cellular growth, programmed cell death, cellular mobility, resistance to chemicals, and tumour development [15]. The overexpression of LINC00261 in colorectal cancer has been demonstrated to alleviate cisplatin resistance by increasing the rate of apoptosis [16]. Similarly, in cases of oesophageal cancer in humans, it was observed that the overexpression of LINC00261 enhanced the responsiveness of tumour cells to 5-fluorouracil (5-FU) medication by controlling the methylation-dependent suppression of dihydropyrimidine dehydrogenase (DYPD) [17]. However, the involvement of only a limited number of lncRNA in the development of PTC has been documented, which leaves the function of LINC00261 in PTC advancement ambiguous.

A substantial body of research has underscored the pivotal role of the lncRNA/miRNA/mRNA axis in a spectrum of ailments, including TC, and has attracted considerable interest from scholars [18,19]. In competitive endogenous RNA, the pairing of lncRNA and miRNA can impede the binding of miRNA to its target genes, thereby regulating the function of target genes [20]. MicroRNA, also referred to as miRNA, is a non-coding RNA comprising 18–22 nucleotides. It is capable of binding with the 3′ untranslated region (3′-UTR) of a specific mRNA molecule, thereby exerting control over the expression of genes. The involvement of miRNA in processes such as cell proliferation, differentiation, metastasis, angiogenesis, and invasion has been well documented in the scientific literature [21]. The role of miR-23a-3p in cancer has been extensively documented in numerous studies on cancer. In renal cell carcinoma (RCC), miR-23a-3p has been demonstrated to enhance the survival, growth, and migration of RCC cell lines [22]. Moreover, the inhibition of LINC00472 in PC has been demonstrated to regulate the proliferation and programmed cell death of PC cells by modulating the activation of BID via miR-23a-3p/FOXO3 pathway [23]. The CELF2 protein is a member of the CELF protein family, and some studies have indicated a potential association with cancer development [24]. It has been demonstrated that the expression of CELF2 is reduced in human breast cancer [25] and colon cancer [26]. However, there is a paucity of information regarding the mechanism of action of miR-23a-3p and CELF2 in PTC.

The objective of the study was to explore the effect of LINC00261/miR-23a-3p/CELF2 on the ^{131}I-resistant PTC cells and to substantiate the regulatory axis. Bioinformatics analysis was used to indicate the potential for distinct expression of LINC00261 in PTC, a hypothesis that was subsequently confirmed in cell lines. Our findings indicate that LINC00261 plays a significant role in the malignant progression of PTC. It is noteworthy that LINC00261 has the capacity to influence miR-23a-3p through targeted regulation. Consequently, the present investigation was undertaken to develop PTC cells and mice resistant to ^{131}I, with the objective of gaining deeper insights into the functional involvement and potential regulatory mechanism of LINC00261 and miR-23a-3p in the malignant advancement of thyroid papillary cancer cells.

2. Materials and methods

2.1. The establishment of cell cultures and the development of cell lines resistant to ^{131}I

The cell line (FTC-133, TPC-1, BCPAP) was purchased from China Wuhan Procell Life Science & Technology Co., Ltd. The cell line (IHH-4) and the human thyroid follicular cell line Nthy-ori 3-1 cells were purchased from China Wuhan Shangen Biotechnology Co., Ltd. The cells were cultivated in RPMI-1640 medium (Sigma-Aldrich, MO, USA) supplemented with 10 % fetal bovine serum (FBS; Gibco, CA, USA) and 1 % double antibody (Sigma-Aldrich). Subsequently, the cells were incubated in a CO_2 cell incubator at 37 °C with 5 % CO_2. The medium for cell culture was replaced every three days, and cells were transferred when the cell density reached 80–90 %. To generate anti-^{131}I cells (TPC-1/R), a continuous supply of the median lethal dose of ^{131}I was introduced to the cell medium with cultured TPC-1 cells for a period of 24 h.

2.2. Transfection and grouping of cells

^{131}I resistant or sensitive cells were transfected with miR-23a-3p mimics, miR-23a-3p inhibitors, and pcDNA3.1 to overexpress CELF2/LINC00261 and sh-LINC00261 (GenePharma, Shanghai, China) using 2 μL Lipofectamine 2000 reagent (Invitrogen Life Technologies). After 24 h, cells were gathered, and TRIzol reagent, along with Ambion® DNase I (Invitrogen Life Technologies), was used to extract total RNA. The successful transfection was confirmed by measuring post-transfection expression levels. The grouping of cell: NC group (TPC-1 cell), TPC-1/R group (TPC-1+IC_{50} of ^{131}I), pcDNA3.1-NC group (TPC-1/R + pcDNA3.1-NC), pcDNA3.1-LINC00261 group (TPC-1/R + pcDNA3.1-LINC00261), sh-NC group (TPC-1/R + sh-NC), sh-LINC00261 group (TPC-1/R + sh-LINC00261), NC mimic group (TPC-1/R + NC mimic), miR-23a-3p mimic group (TPC-1/R + miR-23a-3p mimic), miR-23a-3p inhibitor group (TPC-1/R + miR-23a-3p inhibitor), pcDNA3.1-CELF2 group (TPC-1/R + pcDNA3.1-CELF2), miR-23a-3p mimic + pcDNA3.1-CELF2 group (TPC-1/R + miR-23a-3p mimic + pcDNA3.1-CELF2) and sh-LINC00261+miR-23a-3p inhibitor group (TPC-1/R + sh-LINC00261+miR-23a-3p inhibitor).

2.3. CCK-8 detection

Detection was performed using the CCK-8 test kit (Biyuntian, Beijing, China). The cells were added to a 96-well plate at a concentration of 3×10^3 cells per well and grouped based on the experimental needs, with 3 replicated wells in each group. Each group of cells was cultured for 24 h at 37 °C, 5 % CO_2 Cell incubator. Following the experiment's completion as per each group's specifications, the initial culture medium was discarded and replaced with a fresh 100 μL cell culture medium. Subsequently, 10 μL of CCK-8 solution was introduced and incubated at a temperature of 37 °C for 1 h. A plate reader was utilized to measure the absorbance values at 450 nm.

2.4. RT-qPCR

TRIzol™ Reagent (Invitrogen,15596026) was used to extract the total RNA from tissues and cells of each group, which was then reverse transcribed into single-strand complementary DNA (cDNA) using the One Step Prime Script miRNA cDNA Synthesis Kit (Takara, Kyoto, Japan). Follow the manufacturer's instructions for RT-qPCR using the SYBR Green PCR Master Mix from Life Technologies, located in CA, USA. Table 1 displays the arrangement of RT-qPCR primers. The value was calculated using the $2^{-\Delta\Delta Ct}$ method, with GAPDH or U6 as the internal reference.

Table 1
PCR primer sequence.

Genes	Primer	Sequence (5′-3')
LINC00261	forward	5′- AAGACCAGCTCAACCATCGC-3′
	reverse	5′-TGCCATTTCCTGTGAATTGATGA-3′
miR-23a-3p	forward	5′-TCTCATATGCAGGAGCCACCA-3′
	reverse	5′-GCAAGTTGCTGTAGCCTCCTTG-3′
CELF2	forward	5′- AACCAGACCCAGATGCCATTA-3′
	reverse	5′- ACAAACGCACAGCCTCGA-3′
GAPDH	forward	5′-TGACCACAGTCCATGCCATCAC-3′
	reverse	5′-CGCCTGCTTCACCACCTTCTT-3′
U6	forward	5′-CAAATTCGTGAAGCGTTCCA-3′
	reverse	5′-AGTGCAGGGTCCGAGGTATT-3′

2.5. Western blot

The proteins from each group were obtained using RIPA buffer (Sigma-Aldrich, USA) with 1 % protease inhibitor and phosphatase inhibitor. They were then separated using a 10 % SDS-PAGE gel and transferred onto a polyvinylidene fluoride (PVDF) membrane (Millipore, MA, USA). The film was sealed with 5 % skim milk at room temperature for 2 h. Following this, the first antibody was added and incubated overnight at 4 °C. Subsequently, the second antibody with HRP conjugated (1:2000, ab205718, Abcam, UK) was incubated at room temperature for 1 h. Finally, the protein was detected using chemiluminescence. A control was utilized using an antibody against GAPDH (1:1000, ab181602, Abcam, UK). The ECL chemiluminescence solution BD Biosciences developed was used for exposure and observation. At the same time, protein band analysis was performed using Image J. Abcam, UK provided the following primary antibodies: anti-γ-H2AX (1:100000, ab81299), anti-H2AX (1:3000, ab229914), anti-BRCA1 (1:1000, ab191042), anti-DNA-PKcs (phospho S2056, 1:1000, ab32566), anti-CELF2 (1:5000, ab186430).

2.6. Flow cytometry

The cells were washed twice with 1 × PBS and resuspended in 200 μL of PBS. Fixed overnight in 70 % ethanol precooled at -20 °C. The distribution of cell cycle phases was determined using flow cytometry (BD FACSArray, BD) after staining with propidium iodide (PI) solution (BD, Biosciences, USA) for 15 min. Ensure that there are at least 20000 cells before analysis.

The cells were gathered, rinsed twice using PBS, and revived with 200 μL of PBS. The rate of programmed cell death was measured using the Annexin-V-FITC/PI apoptosis kit from Absin, a company based in China. Following the guidelines provided by the producer, 5 μL of Annexin V-FITC and 5 μL of PI were introduced into every well. The mixture was left to incubate for 15 min in a dimly lit chamber, after which apoptosis was identified using FACScan flow cytometry. Respectively sated the horizontal and vertical axes as Annexin V channel and PI channels and drew a cross gate to determine the proportion of different groups of cells.

2.7. Immunofluorescence (IF)

Inoculating the cells onto a 24-well plate was done with a density of 2×10^4 cells per well. Following 24 h, the cells underwent two rounds of washing using phosphate-buffered saline (PBS) and 4 % paraformaldehyde to permeate cells and then sealed with bovine serum albumin for 1 h. Following that, the cells were incubated overnight at 4 °C with an anti-γ-H2AX (1:250, ab81299, Abcam, UK) antibody. The following day, the cells were cultured with appropriate secondary antibodies for 1 h and stained with DAPI. Finally, the discolored cells were examined and captured using a fluorescence microscope (400857, Nikon, Japan).

2.8. Comet assay

A modified method of Viera et al. [27] was used to perform the comet assay with a reagent kit for single-cell gel electrophoresis (Trevigen, Inc, Gaithersburg, MD, USA). Next, the slides were treated with DAPI stain and observed under fluorescent microscopes. Case software was utilized for the measurement and quantitative analysis of comets.

2.9. Database prediction

The TCGA data analysis database, GEPIA2, was utilized to forecast the variation in LINC00261 expression in PTC. Search the bioinformatics website Starbase (https://starbase.sysu.edu.cn/) to query the binding sequence.

2.10. The gene for luciferase reporter is duplicated

Wild-type miR-23a-3p and CELF2 vectors were created by cloning the 3′-UTR of MiR-23a-3p, which has a binding site for LINC00261, and the 3′-UTR of CELF2, which has a binding site for miR-23a-3p, into the PGL3 vector from Promega in the US. Stratagene kit (Stratagene, US) was used to construct mutant (MUT) miR-23a-3p vectors (miR-23a-3p-MUT) and CELF2 vectors (CELF2-MUT). LINC00261, miR-23a-3p mimic, and NC mimic were transfected into the cells and the luciferase reporter gene constructors. Additionally, the cells were co-transferred with the firefly luciferase reporter plasmid to serve as the normal control. After transfection, the cells were gathered after a period of 24 h. The activity was determined using the Double luciferase reporter system (Promega, US).

2.11. Subcutaneous tumour formation experiment

Kunming Medical University's Animal Experimental Center acquired 18 male BALB/c nude mice aged 6 weeks and weighing 18–22 g. These mice were raised in a controlled and sterile environment following the specific pathogen-free (SPF) standard. The environment was maintained at a temperature of 22 ± 1 °C, with a relative humidity of 50 ± 1 %, and a light/dark cycle of 12/12 h. Mice were injected subcutaneously in the back with 5×10^6 TPC-1 cells, TPC-1 cells transfected with sh-NC, and TPC-1 cells transfected with sh-LINC00261, per group had 6 mice. All animal experiments complied with the ARRIVE guidelines and were carried out in accordance with Guidance on the operation of the Animals (Scientific Procedures) Act 1986 and associated guidelines, EU Directive 2010/63 for the protection of animals used for scientific purposes or the NIH (National Research Council) Guide for the Care and Use of Laboratory Animals. The mice's body weight, tumour volume, and morphology were observed following inoculation. The tumour volume was measured every four days by the formula Volume=(Length × Width^2)/2. After a period of five weeks following the injection, the mice were euthanized, and the tumour tissues were extracted to conduct a subsequent experiment.

2.12. Hematoxylin-eosin staining (HE) staining

The tumour tissue was placed in 15 % EDTA and decalcified in a room-temperature shaker for 1 week. After PBS washing, the tumour tissue was gradient dehydrated with ethanol, embedded in paraffin, sliced with the microtome (4 μm), and then stained with a hematoxylin-eosin (HE) staining kit (Beijing Solebao Biotechnology Co., Ltd.). The tissues were examined by light microscope and photographed, and the tissues were statistically analyzed with ImageJ 1.52.

2.13. TUNEL staining

After being rinsed with PBS two times, the tissue samples received an addition of 50 μL TUNEL detection solution, consisting of 2 μL TDT

enzyme and 48 μL fluorescein-labelled dUTP solution. The tissue samples were washed three times in a moist, dark chamber at a temperature of 37 °C. The specimens were sealed using glycerol, examined, and captured with a laser confocal microscope.

2.14. Immunohistochemistry (IHC)

After removing the wax from the tissue and restoring its moisture, antigen repair was performed using a 0.01 m citrate buffer (pH 6.0). Add anti-Ki-67 (1:200, ab16667, Abcam, UK) and anti-CELF2 (1:100, ab186430, Abcam, UK) for a duration of one night at a temperature of 4 °C. Following this, the immunoassay was conducted using HRP secondary antibody and DAB developer. Results The pictures were taken under the microscope (400857 NiKonjinghe Japan).

2.15. Statistical analysis

The paper presents the experimental data as mean standard deviation (mean ± SD). GraphPad Prism 7 was used to analyze and plot all data. For comparing the two groups, t-tests were employed, while a one-way analysis of variance (One-way ANOVA) was utilized for one-factor multi-group comparison. Additionally, Two-way ANOVA was used for pairwise comparison between groups. $P < 0.05$ considered its difference statistically significant.

3. Results

3.1. Differential expression of LINC00261 observed in cases of papillary thyroid carcinoma

Our first step was to predict the differential expression of LINC00261 in PTC using the GEPIA2 database. We found that LINC00261 expression was down-regulated in PTC (Fig. 1 A). In comparison to Nthy-ori 3-1 cells, the TC cell lines exhibited a notable decrease in the expression of LINC00261 (Fig. 1B-C), of which TPC-1 cells were the most significant so that TPC-1 cells will be selected for subsequent experiments.

3.2. Effect of LINC00261 on malignant biological behavior of ^{131}I-sensitive PTC cells

The objective of this study was to investigate the impact of LINC00261 on PTC cells treated with ^{131}I. ^{131}I-resistant PTC cells (TPC-1/R) were established by subjecting TPC-1 to a prolonged exposure of ^{131}I at a sublethal dose. The findings indicated that the IC_{50} value of ^{131}I in TPC-1/R cells exhibited a more than two-fold increase in comparison to normal TPC-1 cells (Fig. 2 A). Subsequently, pcDNA3.1-NC, pcDNA3.1-LINC00261, sh-NC, and sh-LINC00261 were introduced into the cells through additional transfection. The RT-qPCR detection results indicated no notable disparity in the expression of LINC00261 between the pcDNA3.1-NC and sh-NC groups in comparison to the TPC-1/R group. However, the expression of LINC00261 in the pcDNA3.1-LINC00261 group was significantly greater than that observed in the sh-LINC00261 group (Fig. 2 B), indicating that the transfection was successful. Additional analysis of cell viability and apoptosis revealed that compared to the NC group, the TPC-1/R group demonstrated a suppression of cell proliferation and the S phase while an enhancement of apoptosis. Moreover, the pcDNA3.1-LINC00261 group further demonstrated a greater inhibitory effect on cell proliferation and the S phase, while promoting cell apoptosis compared to the TPC-1/R group. In contrast, the sh-LINC00261 group exhibited a notable stimulation of cell proliferation and the S phase while apoptosis was inhibited (Fig. 2C-E). The genomes of tumour cells are characteristically unstable, and the role of DNA damage-induced apoptosis in PTC, which impedes tumour growth, is of paramount importance [28]. The IF and Western blot analyses were conducted to detect theγ-H2AX, BRCA1, and DNA-PKcs, which are the markers of the DNA damage response. The findings indicated that compared to the TPC-1/R group, the pcDNA3.1-LINC00261 group exhibited a notable increase in γ-H2AX expression and a significant decrease in BRCA1 and DNA-PKcs protein expression. Conversely, the sh-LINC00261 group demonstrated a notable reduction in γ-H2AX expression and a significant increase in BRCA1 and DNA-PKcs protein expression (Fig. 2F-H). The comet assay was employed to identify DNA double-strand breaks. An increase in the size of the comet's tail is indicative of a greater degree of DNA damage. In comparison to the TPC-1/R group, the pcDNA3.1-LINC00261 group demonstrated a notable increase in tail length, whereas the sh-LINC00261 group exhibited a significant reduction in tail length (Fig. 2 G). The results demonstrate that pcDNA3.1-LINC00261 can impede the malignant progression of TPC-1/R cells and can be reversed by sh-LINC00261.

3.3. LINC00261 regulates the expression of miR-23a-3p, which in turn regulates the expression of CELF2

To investigate the functioning of LINC00261 in PTC, the presence of binding sites between LINC00261 and miR-23a-3p was identified in the

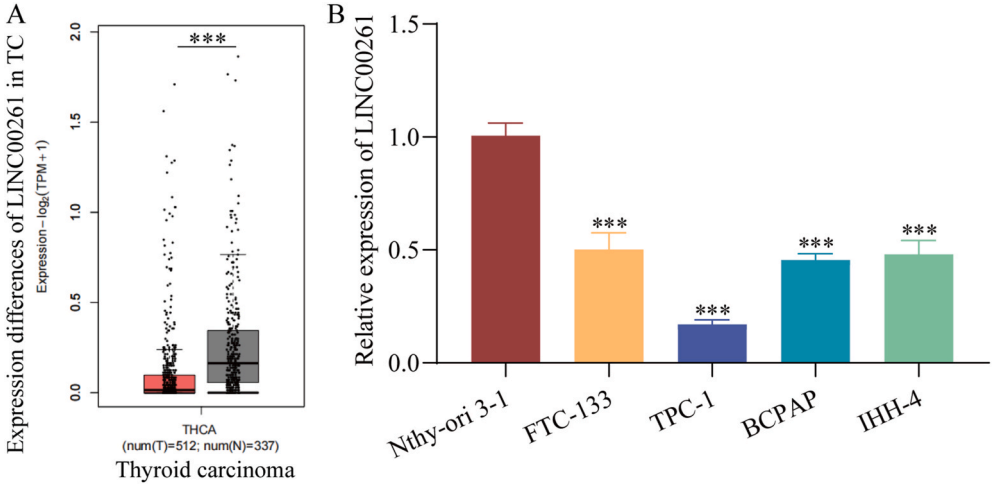

Fig. 1. Differential expression of LINC00261 in PTC. A: The database predicted the differential expression of LINC00261 in PTC. B: RT-qPCR was used to detect the expression of LINC00261 in TC cell lines (FTC-133, TPC-1, BCPAP, and IHH-4) and human thyroid follicular cell line Nthy-ori 3-1. ***$P < 0.001$, compared with Nthy-ori 3-1, n = 3.

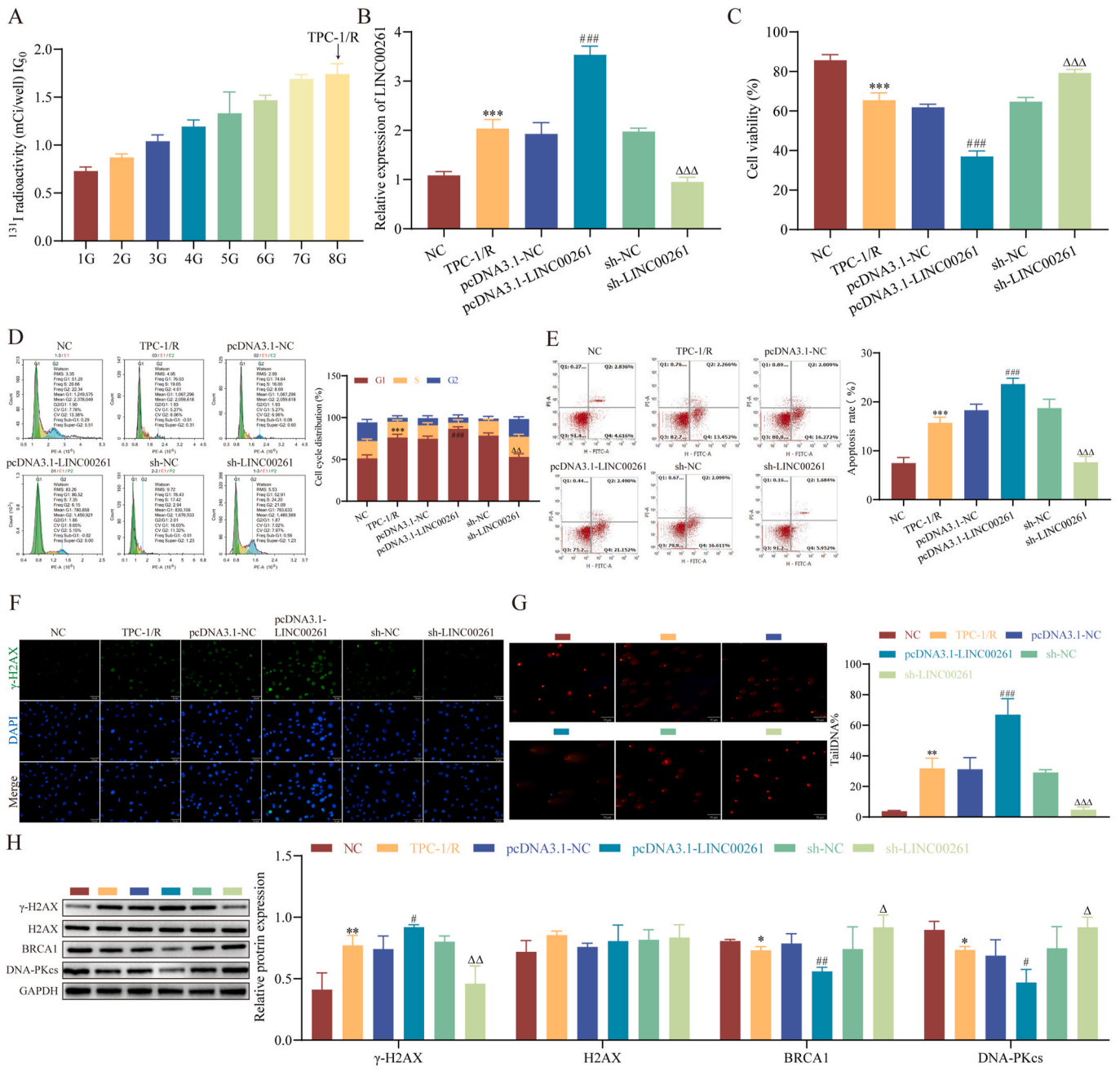

Fig. 2. Effect of LINC00261 on malignant biological behavior of ^{131}I-sensitive PTC cells. A: IC_{50} value detected by CCK-8. B: Detection of transfection efficiency of LINC00261 by RT-qPCR. C: CCK-8 detection of TPC-1/R cell proliferation. D-E: Flow cytometry detection of TPC-1/R cell cycle and cell apoptosis. F: Detection of focus formation of γ-H2AX by IF, Scale bar = 20 μm. G: Comet assay, Scale bar = 50 μm. H: Western blot to detect the expression of DNA damage markers γ-H2AX and H2AXMagne BRCA1 and DNA-PKcs; compared with NC group, $^{*}P < 0.05$, $^{**}P < 0.01$, $^{***}P < 0.001$; compared with TPC-1/R group, $^{\#}P < 0.05$, $^{\#\#}P < 0.01$, $^{\#\#\#}P < 0.001$; compared with pcDNA3.1-LINC00261 group, $^{\Delta}P<0.05$, $^{\Delta\Delta}P<0.01$, $^{\Delta\Delta\Delta}P<0.001$, n = 3.

Starbase database. Additionally, miR-23a-3p and CELF2 (Fig. 3 A). The co-transfection comprised the introduction of a miR-23a-3p mimic in conjunction with LINC00261-MUT, LINC00261-wild type (WT), CELF2-MUT, and CELF2-WT. The results demonstrated that the elevated expression of miR-23a-3p resulted in a considerable decline in the relative luciferase activity of the LINC00261-WT and CELF2-WT vectors. However, this did not result in a notable impact on the mutant vector's relative luciferase activity (Fig. 3 B). Consequently, pcDNA3.1-LINC00261 and sh-LINC00261 were transfected to detect the expression of miR-23a-3p. The RT-qPCR result demonstrated that the expression of miR-23a-3p was down-regulated by pcDNA3.1-LINC00261, while the opposite result was observed with sh-LINC00261 (Fig. 3C). Subsequently, the cellular environment was assessed to determine the impact of miR-23a-3p overexpression or suppression on CELF2 protein expression. The findings indicated that compared to the NC group, the group treated with the miR-23a-3p mimic exhibited a significant reduction in the expression level of CELF2. In contrast, the group treated with the miR-23a-3p inhibitor demonstrated a significant increase in CELF2 expression (Fig. 3 D). These results indicated that LINC00261 targeted and negatively regulated the miR-23a-3p expression, while miR-23a-3p targeted and negatively regulated the CELF2 protein expression.

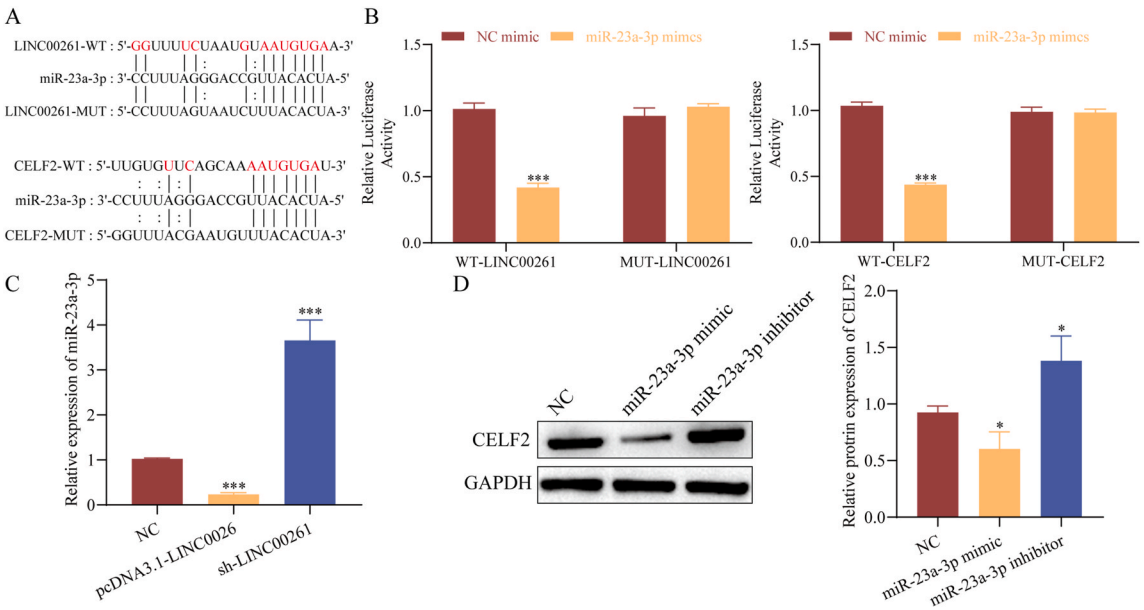

Fig. 3. LINC00261 targeted regulation of miR-23a-3p expression, miR-23a-3p targeted regulation of CELF2 expression. A: miR-23a-3p binding sequence with LINC00261 and CELF2. B: Double luciferase gene reporting verifies. C: RT-qPCR detected the expression level of miR-23a-3p and LINC00261. D: Western blot detected the expression level of CELF2 protein after expression and knockdown of miR-23a-3p. $^{*}P < 0.05$, $^{***}P < 0.001$, compared with NC group, n = 3.

3.4. Effect of LINC00261 on malignant biological behavior of ^{131}I-sensitive PTC cells through miR-23a-3p/CELF2

To delve deeper into the molecular mechanism by which LINC00261 exerts its influence on TPC-1/R cells via the miR-23a-3p/CELF2 axis. We co-transfection the miR-23a-3p inhibitor/mimic, pcDNA3.1-CELF2, and sh-LINC00261 into the cells. In comparison to the TPC-1/R group, the miR-23a-3p inhibitor group demonstrated a notable decline miR-23a-3p expression and an increase in CELF2 expression, as evidenced by RT-qPCR analysis. The pcDNA3.1-CELF2 group further increased the expression of miR-23a-3p, yet did not exert a notable impact on CELF2 expression. However, co-transfection of the miR-23a-3p mimic + pcDNA3.1-CELF2 group resulted in a notable elevation in miR-23a-3p expression and a reduction in CELF2 expression. In conclusion, the co-transfection sh-LINC00261+miR-23a-3p inhibitor group demonstrated a significant decrease in miR-23a-3p expression and increased CELF2 expression, as illustrated in Fig. 4A and B. Further assessment of cell viability and programmed cell death revealed that the miR-23a-3p inhibitor group impeded cell growth and the S phase while enhancing cell apoptosis compared to the TPC-1/R group. No notable distinction was observed between the pcDNA3.1-CELF2 and miR-23a-3p inhibitor groups. In contrast, the miR-23a-3p mimic + pcDNA3.1-CELF2 group and the sh-LINC00261+miR-23a-3p inhibitor group demonstrated a notable stimulation of cell growth and the S phase, while apoptosis was suppressed (Fig. 4C-E). In comparison to the TPC-1/R group, the knockdown miR-23a-3p resulted in a notable elevation in γ-H2AX expression and a pronounced reduction in BRCA1 and DNA-PKcs protein expression. Conversely, the pcDNA3.1-CELF2 group demonstrated no statistically significant differences. Furthermore, the miR-23a-3p mimic + pcDNA3.1-CELF2 group and sh-LINC00261+miR-23a-3p inhibitor group exhibited a notable reduction in γ-H2AX expression, accompanied by an increase in BRCA1 and DNA-PKcs protein expression (Fig. 4F-H). The comet assay was employed to detect DNA damage, compared to the miR-23a-3p inhibitor group, no significant difference was observed in the tail length of the pcDNA3.1-CELF2 group. Conversely, the tail length of the miR-23a-3p mimic + pcDNA3.1-CELF2 group and sh-LINC00261+miR-23a-3p inhibitor group was significantly reduced (Fig. 4 G). The results demonstrated that LINC00261 inhibits the malignant progression of TPC-1/R cells through the modulation of the miR-23a-3p/CELF2 pathway.

3.5. Verification of the effect of LINC00261 on tumourigenicity of TPC-1 cells in vivo

To elucidate the function of LINC00261 in PTC more comprehensively, we transfected sh-NC and sh-LINC00261 into cells and conducted subcutaneous xenotransplantation experiments. The findings indicated no notable disparity in the mice's body weight across all groups, and the tumour mass between the sh-NC group and the Control group exhibited no significant distinction. However, the sh-LINC00261 group exhibited a notable acceleration in tumour growth, as illustrated in Fig. 5A-B. The results of the HE, TUNEL, and IHC assay indicated that there were no notable differences between sh-NC and Control groups. Nevertheless, the inhibition of LINC00261 markedly accelerated tumour progression and Ki-67 manifestation and hindered CELF2 expression and apoptosis (Fig. 5C-E). Additionally, the introduction of sh-LINC00261 was observed to effectively suppress the levels of CELF2 and γ-H2AX while enhancing the levels of BRCA1 and DNA-PKcs, as demonstrated by the findings from IF and Western blot analysis (Fig. 5F-G). The RT-qPCR analysis demonstrated that the introduction of sh-LINC00261 considerably suppressed the presence of LINC00261 while enhancing the presence of miR-23a-3p (Fig. 5H). The results demonstrated that the silencing of LINC00261 can facilitate the progression of PTC via the miR-23a-3p/CELF2 pathway.

4. Discussion

Papillary thyroid carcinoma (PTC) represents 80 % of all malignant tumours in the thyroid, making it the most prevalent malignant tumour in the endocrine gland. The principal clinical treatment strategies for PTC are surgery and ^{131}I radiotherapy. As the incidence of PTC continues to rise, the postoperative recurrence rate and metastasis rates for PTC patients are relatively high, and the sensitivity to chemotherapy is low [29]. It is therefore vital to investigate the molecular mechanism of PTC, as this will facilitate the development of more effective therapies. A substantial body of research has demonstrated that LncRNA plays a pivotal role in regulating the response to medication in PTC. This is the first demonstration that PTC cells display reduced levels of LINC00261

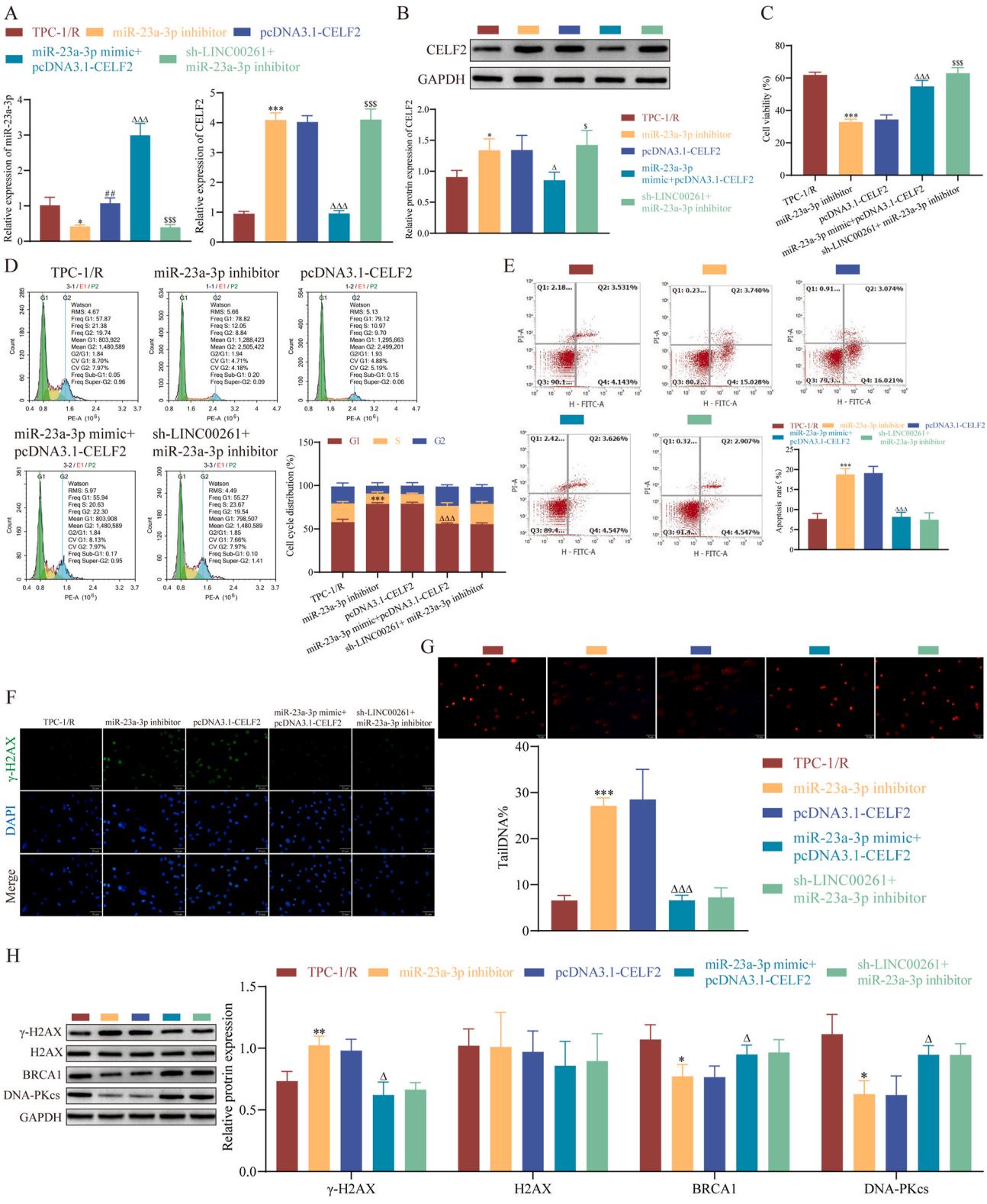

Fig. 4. Effect of LINC00261 on malignant biological behavior of TPC-1/R cells through miR-23a-3p/CELF2. A: The expression of miR-23a-3p and CELF2 in each group. B: Western blot detected the expression of CELF2 in each group. C: CCK-8 detection of TPC-1/R cell proliferation. D-E: Flow cytometry detection of TPC-1/R cell cycle and cell apoptosis. F: Detection of focus formation of γ-H2AX by IF, Scale bar = 20 μm. G: Detection of DNA damage by comet assay, Scale bar = 50 μm. H: The expression of DNA damage markers γ-H2AX and H2AXMagne BRCA1 and DNA-PKcs; compared with TPC-1/R group, $^{*}P < 0.05$, $^{**}P < 0.01$, $^{***}P < 0.001$; compared with miR-23a-3p inhibitor group, $^{\#}P < 0.05$, $^{\#\#}P < 0.01$, $^{\#\#\#}P < 0.001$; compared with pcDNA3.1-CELF2 group, $^{\Delta}P<0.05$, $^{\Delta\Delta}P<0.01$, $^{\Delta\Delta\Delta}P<0.001$; compared with miR-23a-3p mimic + pcDNA3.1-CELF2 group, $^{\$}P < 0.05$, $^{\$\$}P < 0.01$, $^{\$\$\$}P < 0.001$, n = 3.

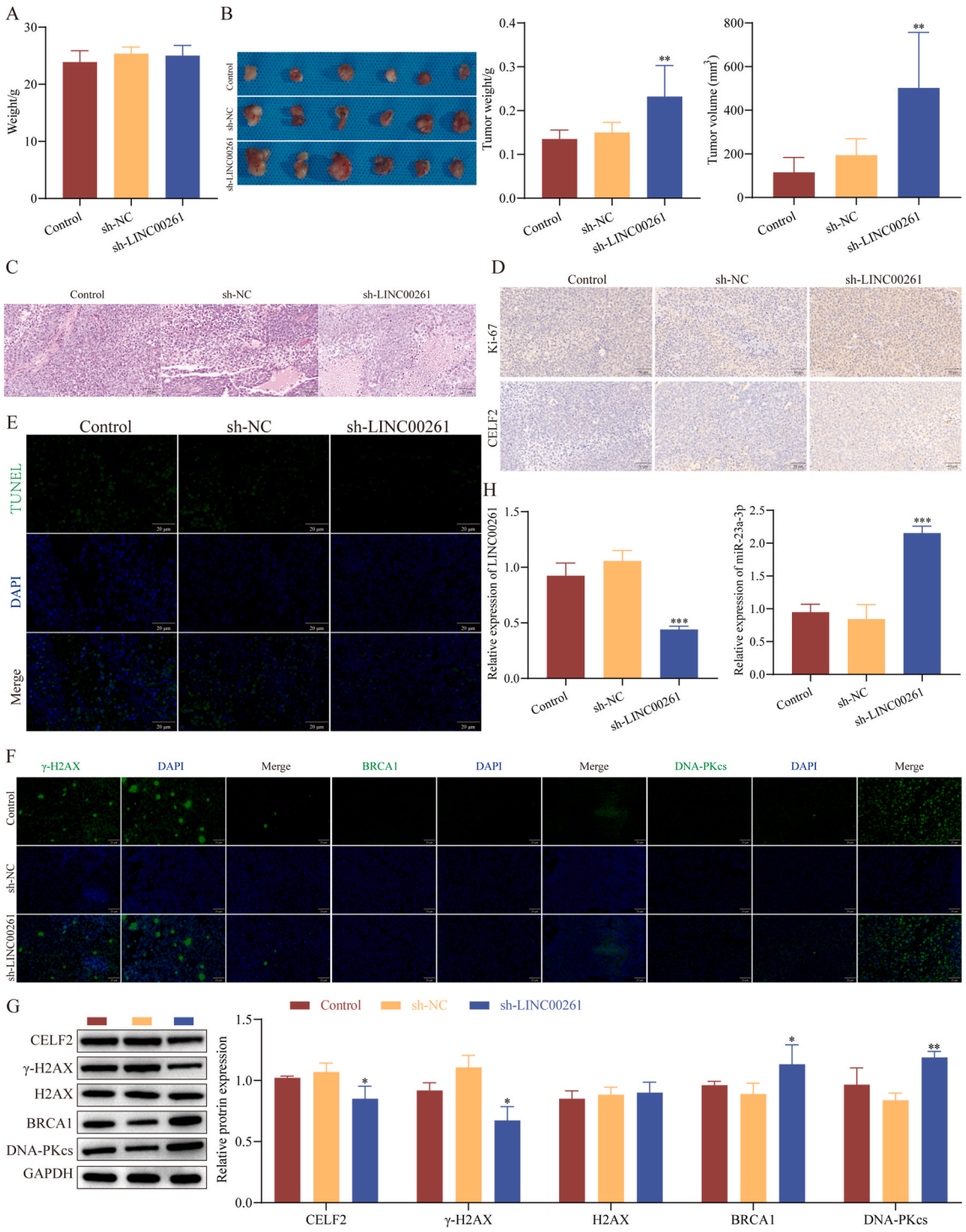

Fig. 5. Verification of the effect of LINC00261 on tumourigenicity of TPC-1 cells in vivo. A: Mouse body weight. B: Tumour volume and weight. C: HE staining, Scale bar = 50 μm. D: Detection of Ki-67 and CELF2 by IHC, Scale bar = 50 μm. E: Detection of apoptosis by TUNEL staining, Scale bar = 20 μm. F: IF detection of the expression of γ-H2AX (S139), BRCA1, and DNA-PKcs. G: Western blot detection of CELF2, γ-H2AX, and H2AXJING BRCA1 and DNA-PKcs protein expression, Scale bar = 20 μm. H: RT-qPCR detect. $^{*}P < 0.05$, $^{**}P < 0.01$, $^{***}P < 0.001$, n = 6.

expression. LINC00261 has been demonstrated to regulate the proliferation and arrest of the cell cycle in ^{131}I-resistant PTC cells, as well as promote apoptosis by inducing DNA damage.

The role of lncRNA in various cellular and physiological activities, particularly in controlling tumour development and progression, has been demonstrated. Several lncRNA have been documented to be aberrantly expressed in various types of cancer and to control cancer cell growth, development, cell death, migration and infiltration [30,31]. In TC, various lncRNAs have been identified as influential elements in the a progression of TC. This lncRNA can serve as an early detection tool and a potential biomarker for biotherapy [32]. In their study, Huo and colleagues discovered that LINC00671 inhibits glucose uptake, growth, movement, and knockdown of LDHA to promote PTC death. LINC00671 may be a promising therapeutic approach for the treatment of TC [33]. However, the use of LINC00261 in PTC remains uncertain. The expression of LINC00261 was significantly reduced in PC tissues, mainly

localised in the nucleus, and its overexpression suppressed PC cell invasion and migration [34]. Cheng and colleagues conducted a study and found that the levels of LncRNA-SLC6 A9 were reduced in patients who were insensitive to ^{131}I treatment and in PC cells that were resistant to ^{131}I. Increasing the expression of SLC6 A9 positively regulated poly ADP-ribose polymerase 1 (PARP-1), thereby increasing the responsiveness of PTC cells to ^{131}I therapy [4]. Consistent with this, we verified that LINC00261 levels were reduced in both PTC tissues and cells. LINC00261 suppressed the proliferation and S-phase of ^{131}I-resistant PTC cells, while enhancing apoptosis. It is well known that DNA damage is a primary factor in tumourigenesis. The primary approach to treating TC in a clinical setting involves ^{131}I exposure, which leads to the induction of various forms of DNA damage [35]. DNA repair can inhibit tumour progression. The level of activation of most of the differential pathways has been found to be significantly up-regulated in papillary carcinoma, whereas it is moderately up-regulated in follicular carcinoma. In radioiodine-resistant thyroid tumours, BRCA1, as a critical factor in the activation of DNA repair, has been confirmed to improve the treatment of different types of TC, thus helping to find other markers of ^{131}I resistance [28]. Apoptosis and cell cycle arrest occur when mammalian cells are unable to repair DNA damage, leading to the activation of DNA damage [36]. In Wu et al. research, the use of recombinant adenovirus-p53 (rAd-p53) demonstrated effective tumour suppression and increased sensitivity to paclitaxel (PTX), a chemotherapeutic drug for PTC. This was achieved by activating DNA damage, inducing apoptosis, causing S-arrest and inhibiting cell proliferation in PTC cells in the laboratory and in living organisms [37]. The results of our study showed that pcDNA3.1-LINC00261 induced apoptosis and caused S-phase arrest in TPC-1/R cells by increasing the levels of γ-H2AX, reducing the levels of BRCA1 and DNA-PKcs, and activating DNA damage.

The involvement of the lncRNA/miRNA/mRNA pathway in the aetiology of a number of diseases, including TC, has been the subject of extensive investigation. The coexistence of lncRNA and miRNA can impede the binding of miRNA to its target genes, consequently modulating the functionality of said target genes [38]. It was discovered thatImmunogastroenterologycan regulate the expression of miR-23a-3p, subsequently acting on downstream proteins CELF2 and exerting a negative regulatory effect. It has been reported that circRNA_103598 binds with miR-23a-3p to enhance cell proliferation in PTC by regulating the direct target IL-6 [39]. The overexpression of miR-23a-3p was observed to enhance the survival, growth, and motility of RCC cells while simultaneously inhibiting apoptosis [22]. As reported by Sabirzhanov et al., miR-23a-3p has been shown to induce apoptosis. A further reduction in the level of miR-23a-3p results in the activation of DNA damage in neurons, which in turn causes neuronal apoptosis [40]. The CELF2 gene is located chromosome 10p. The CELF2 gene has been demonstrated to function as a tumour suppressor, with its frequent deletion in multiple cancers [41]. The downregulation of CELF2 is a highly significant factor in the development of ovarian cancer. The overexpression of CELF2 has been demonstrated to impede the proliferation, migration, and malignant progression of ovarian tumour cells in vitro and in vivo [42]. The results of our study demonstrate that the inhibition of LINC00261, both in vitro and in vivo, can promote cellular proliferation, inhibit programmed cell death, and facilitate the progression of PTC by inhibiting DNA damage through the miR-23a-3p/CELF2 pathway.

In conclusion, LINC00261, which acts as a tumour suppressor, is capable of regulating a multitude of biological processes associated with cancer. The results of this study demonstrated that the levels of LINC00261 were significantly decreased in both PTC tissues and cells. The inhibition of LINC00261 impairs DNA damage by regulating the miR-23a-3p/CELF2 pathway, which also inhibits apoptosis and S-phase arrest in ^{131}I-resistant PTC cells and promotes the malignant progression of PTC in vivo and in vitro. Hence, the results of this study suggest that LINC00261 may serve as a potential target for the clinical management of PTC and ^{131}I therapy in PTC patients. As ^{131}I was not employed in this study at the animal level, it is essential to provide further clarification regarding the impact of LINC00261 on ^{131}I in the management of PTC through in vivo and clinical investigations.

CRediT authorship contribution statement

Qingyuan Tao: Writing – original draft, Validation. **Xiaojin Li:** Writing – original draft, Formal analysis, Data curation. **Yanyan Xia:** Validation. **Bin Zheng:** Validation, Resources. **Yijun Yan:** Formal analysis. **Songrun Wang:** Resources. **Li Jia:** Writing – review & editing, Conceptualization.

Ethical approval

The animal experiments with the assistance of Yunnan Labreal Biotech Co., Ltd., the animal experiment were conducted and received approval from the Experimental Animal Ethics Committee of Yunnan Labreal Biotech Co., Ltd. (IACUC Issue No. PZ20221002).

Data availability statement

Data is applicable after the approval of co-authors.

Funding information

In this study, no funding was received.

Declaration of competing interest

All authors declare that they have no conflict of interest.

Appendix A. Supplementary data

Supplementary data to this article can be found online at https://doi.org/10.1016/j.bbrep.2024.101858.

References

[1] R.L. Siegel, K.D. Miller, A. Jemal, Cancer statistics, 2019, CA A Cancer J. Clin. 69 (1) (2019) 7–34, https://doi.org/10.3322/caac.21551.
[2] F. Ambrosi, A. Righi, C. Ricci, et al., Hobnail variant of papillary thyroid carcinoma: a literature review, Endocr. Pathol. 28 (4) (2017) 293–301, https://doi.org/10.1007/s12022-017-9502-7.
[3] D. Liu, S. Hu, P. Hou, et al., Suppression of BRAF/MEK/MAP kinase pathway restores expression of iodide-metabolizing genes in thyroid cells expressing the V600E BRAF mutant, Clin. Cancer Res. 13 (4) (2007) 1341–1349, https://doi.org/10.1158/1078-0432.Ccr-06-1753.
[4] C. Xiang, M.L. Zhang, Q.Z. Zhao, et al., LncRNA-SLC6A9-5:2: a potent sensitizer in 131I-resistant papillary thyroid carcinoma with PARP-1 induction, Oncotarget 8 (14) (2017) 22954–22967, https://doi.org/10.18632/oncotarget.14578.
[5] Z. Xiping, C. Bo, Y. Shifeng, et al., Roles of MALAT1 in development and migration of triple negative and Her-2 positive breast cancer, Oncotarget 9 (2) (2018) 2255–2267, https://doi.org/10.18632/oncotarget.23370.
[6] L. Shi, Y.Z. Cong, Z.J. Wang, LncRNA NORAD promotes thyroid carcinoma progression by targeting miR-451, Eur. Rev. Med. Pharmacol. Sci. 25 (20) (2021) 6187–6195, https://doi.org/10.26355/eurrev_202110_26989.
[7] W.X. Peng, P. Koirala, Y.Y. Mo, LncRNA-mediated regulation of cell signaling in cancer, Oncogene 36 (41) (2017) 5661–5667, https://doi.org/10.1038/onc.2017.184.
[8] Z. Javed, F. Ahmed Shah, S. Rajabi, et al., LncRNAs as potential therapeutic targets in thyroid cancer, Asian Pac. J. Cancer Prev. APJCP 21 (2) (2020) 281–287, https://doi.org/10.31557/apjcp.2020.21.2.281.
[9] F. Shi, Y. Liu, M. Li, et al., Analysis of lncRNA and mRNA transcriptomes expression in thyroid cancer tissues among patients with exposure of medical occupational radiation, Dose Response 17 (3) (2019) 1559325819864223, https://doi.org/10.1177/1559325819864223.
[10] M.D. Story, M. Durante, Radiogenomics, Med. Phys. 45 (11) (2018) e1111–e1122, https://doi.org/10.1002/mp.13064.
[11] Y. Liu, P. Yue, T. Zhou, et al., LncRNA MEG3 enhances (131)I sensitivity in thyroid carcinoma via sponging miR-182, Biomed. Pharmacother. 105 (2018) 1232–1239, https://doi.org/10.1016/j.biopha.2018.06.087.
[12] S. Müller, S. Raulefs, P. Bruns, et al., Next-generation sequencing reveals novel differentially regulated mRNAs, lncRNAs, miRNAs, sdRNAs and a piRNA in

pancreatic cancer, Mol. Cancer 14 (2015) 94, https://doi.org/10.1186/s12943-015-0358-5.
[13] W.J. Cao, H.L. Wu, B.S. He, et al., Analysis of long non-coding RNA expression profiles in gastric cancer, World J. Gastroenterol. 19 (23) (2013) 3658–3664, https://doi.org/10.3748/wjg.v19.i23.3658.
[14] Y. Liu, N. Xiao, S.F. Xu, Decreased expression of long non-coding RNA LINC00261 is a prognostic marker for patients with non-small cell lung cancer: a preliminary study, Eur. Rev. Med. Pharmacol. Sci. 21 (24) (2017) 5691–5695, https://doi.org/10.26355/eurrev_201712_14014.
[15] M. Zhang, F. Gao, X. Yu, et al., LINC00261: a burgeoning long noncoding RNA related to cancer, Cancer Cell Int. 21 (1) (2021) 274, https://doi.org/10.1186/s12935-021-01988-8.
[16] Z.K. Wang, L. Yang, L.L. Wu, et al., Long non-coding RNA LINC00261 sensitizes human colon cancer cells to cisplatin therapy, Braz. J. Med. Biol. Res. 51 (2) (2017) e6793, https://doi.org/10.1590/1414-431x20176793.
[17] K. Lin, H. Jiang, S.S. Zhuang, et al., Long noncoding RNA LINC00261 induces chemosensitization to 5-fluorouracil by mediating methylation-dependent repression of DPYD in human esophageal cancer, Faseb. J. 33 (2) (2019) 1972–1988, https://doi.org/10.1096/fj.201800759R.
[18] K. Guo, K. Qian, Y. Shi, et al., LncRNA-MIAT promotes thyroid cancer progression and function as ceRNA to target EZH2 by sponging miR-150-5p, Cell Death Dis. 12 (12) (2021) 1097, https://doi.org/10.1038/s41419-021-04386-0.
[19] D. Bai, C. Guo, A. Wang, et al., LncRNA CASC15 promotes the proliferation of papillary thyroid carcinoma cells by regulating the miR-7151-5p/WNT7A axis, Pathol. Res. Pract. 225 (2021) 153561, https://doi.org/10.1016/j.prp.2021.153561.
[20] X. Qi, D.H. Zhang, N. Wu, et al., ceRNA in cancer: possible functions and clinical implications, J. Med. Genet. 52 (10) (2015) 710–718, https://doi.org/10.1136/jmedgenet-2015-103334.
[21] Y. Zhang, C. Chen, Z. Liu, et al., PABPC1-induced stabilization of IFI27 mRNA promotes angiogenesis and malignant progression in esophageal squamous cell carcinoma through exosomal miRNA-21-5p, J. Exp. Clin. Cancer Res. 41 (1) (2022) 111, https://doi.org/10.1186/s13046-022-02339-9.
[22] J. Quan, X. Pan, Y. Li, et al., MiR-23a-3p acts as an oncogene and potential prognostic biomarker by targeting PNRC2 in RCC, Biomed. Pharmacother. 110 (2019) 656–666, https://doi.org/10.1016/j.biopha.2018.11.065.
[23] C. Bi, G. Wang, LINC00472 suppressed by ZEB1 regulates the miR-23a-3p/FOXO3/BID axis to inhibit the progression of pancreatic cancer, J. Cell Mol. Med. 25 (17) (2021) 8312–8328, https://doi.org/10.1111/jcmm.16784.
[24] J. Li, L. Xian, Z. Zhu, et al., Role of CELF2 in ferroptosis: potential targets for cancer therapy (review), Int. J. Mol. Med. 52 (4) (2023), https://doi.org/10.3892/ijmm.2023.5291.
[25] L. Piqué, A. Martinez De Paz, D. Piñeyro, et al., Epigenetic inactivation of the splicing RNA-binding protein CELF2 in human breast cancer, Oncogene 38 (45) (2019) 7106–7112, https://doi.org/10.1038/s41388-019-0936-x.
[26] S. Ramalingam, P. Ramamoorthy, D. Subramaniam, et al., Reduced expression of RNA binding protein CELF2, a putative tumor suppressor gene in colon cancer, Immunogastroenterol. 1 (1) (2012) 27–33, https://doi.org/10.7178/ig.1.1.7.
[27] T. Viera, P.L. Patidar, DNA damage induced by KP372-1 hyperactivates PARP1 and enhances lethality of pancreatic cancer cells with PARP inhibition, Sci. Rep. 10 (1) (2020) 20210, https://doi.org/10.1038/s41598-020-76850-4.
[28] U. Vladimirova, P. Rumiantsev, M. Zolotovskaia, et al., DNA repair pathway activation features in follicular and papillary thyroid tumors, interrogated using 95 experimental RNA sequencing profiles, Heliyon 7 (3) (2021) e06408, https://doi.org/10.1016/j.heliyon.2021.e06408.
[29] M.F. Bates, M.R. Lamas, R.W. Randle, et al., Back so soon? Is early recurrence of papillary thyroid cancer really just persistent disease? Surgery 163 (1) (2018) 118–123, https://doi.org/10.1016/j.surg.2017.05.028.
[30] L. Statello, C.J. Guo, L.L. Chen, et al., Gene regulation by long non-coding RNAs and its biological functions, Nat. Rev. Mol. Cell Biol. 22 (2) (2021) 96–118, https://doi.org/10.1038/s41580-020-00315-9.
[31] B. Zhou, H. Yang, C. Yang, et al., Translation of noncoding RNAs and cancer, Cancer Lett. 497 (2021) 89–99, https://doi.org/10.1016/j.canlet.2020.10.002.
[32] M.R. Mahmoudian-Sani, A. Jalali, M. Jamshidi, et al., Long non-coding RNAs in thyroid cancer: implications for pathogenesis, diagnosis, and therapy, Oncol. Res. Treat. 42 (3) (2019) 136–142, https://doi.org/10.1159/000495151.
[33] N. Huo, R. Cong, Z.J. Sun, et al., STAT3/LINC00671 axis regulates papillary thyroid tumor growth and metastasis via LDHA-mediated glycolysis, Cell Death Dis. 12 (9) (2021) 799, https://doi.org/10.1038/s41419-021-04081-0.
[34] B. Li, S. Pang, J. Dou, et al., The inhibitory effect of LINC00261 upregulation on the pancreatic cancer EMT process is mediated by KLF13 via the mTOR signaling pathway, Clin. Transl. Oncol. 24 (6) (2022) 1059–1072, https://doi.org/10.1007/s12094-021-02747-x.
[35] J. Wadsley, N. Armstrong, V. Bassett-Smith, et al., Patient preparation and radiation protection guidance for adult patients undergoing radioiodine treatment for thyroid cancer in the UK, Clin. Oncol. 35 (1) (2023) 42–56, https://doi.org/10.1016/j.clon.2022.07.002.
[36] P. Strzyz, DNA damage response: cell thriving despite DNA damage, Nat. Rev. Mol. Cell Biol. 17 (7) (2016) 396, https://doi.org/10.1038/nrm.2016.86.
[37] W. Wu, T. Wei, Z. Li, et al., p53-dependent apoptosis is essential for the antitumor effect of paclitaxel response to DNA damage in papillary thyroid carcinoma, Int. J. Med. Sci. 18 (14) (2021) 3197–3205, https://doi.org/10.7150/ijms.61944.
[38] H. Liu, H. Deng, Y. Zhao, et al., LncRNA XIST/miR-34a axis modulates the cell proliferation and tumor growth of thyroid cancer through MET-PI3K-AKT signaling, J. Exp. Clin. Cancer Res. 37 (1) (2018) 279, https://doi.org/10.1186/s13046-018-0950-9.
[39] S. Zhang, Q. Wang, D. Li, et al., Oncolytic vaccinia virus-mediated antitumor effect and cell proliferation were promoted in PTC by regulating circRNA_103598/miR-23a-3p/IL-6 Axis, Cancer Manag. Res. 12 (2020) 10389–10396, https://doi.org/10.2147/cmar.S273072.
[40] B. Sabirzhanov, O. Makarevich, J. Barrett, et al., Down-regulation of miR-23a-3p mediates irradiation-induced neuronal apoptosis, Int. J. Mol. Sci. 21 (10) (2020), https://doi.org/10.3390/ijms21103695.
[41] A. Al-Ibraheemi, A. Martinez, S.W. Weiss, et al., Fibrous hamartoma of infancy: a clinicopathologic study of 145 cases, including 2 with sarcomatous features, Mod. Pathol. 30 (4) (2017) 474–485, https://doi.org/10.1038/modpathol.2016.215.
[42] Q. Guo, Y. Wu, X. Guo, et al., The RNA-binding protein CELF2 inhibits ovarian cancer progression by stabilizing FAM198B, Mol. Ther. Nucleic Acids 23 (2021) 169–184, https://doi.org/10.1016/j.omtn.2020.10.011.